

ABSTRACT

Breast cancer is a fatal disease that has a high rate of morbidity and mortality. Finding the right diagnosis is one of the most crucial steps in breast cancer treatment. Doctors can use machine learning (ML) and deep learning techniques to aid with diagnosis. This work makes an effort to devise a methodology for the classification of Breast cancer into its molecular subtypes and prediction of relapse. The objective is to compare the performance of Deep CNN, Tuned CNN and Hypercomplex-Valued CNN, and infer the results, thus automating the classification process. The traditional method used by doctors to detect is tedious and time consuming. It employs multiple methods, including MRI, CT scanning, aspiration, and blood tests as well as image testing. The proposed approach uses image processing techniques to detect irregular breast tissues in the MRI. The survivors of Breast Cancer are still at risk for relapse after remission, and once the disease relapses, the survival rate is much lower. A thorough analysis of data can potentially identify risk factors and reduce the risk of relapse in the first place. A SVM (Support Vector Machine) module with GridSearchCV for hyperparameter tuning is used to identify patterns in those patients who experience a relapse, so that these patterns can be used to predict the relapse before it occurs.

TABLE OF CONTENTS

ABSTRACT	iii
LIST OF TABLES	vii
LIST OF FIGURES	viii
1 INTRODUCTION	1
1.1 MOTIVATION	1
1.2 BACKGROUND	2
1.2.1 Factors Contributing to Breast Cancer	2
1.2.2 Staging of Breast Cancer	6
1.3 PROBLEM DEFINITION	9
1.4 ORGANIZATION OF THE REPORT	9
2 LITERATURE SURVEY	11
2.1 PAPERS RELATED TO THE PROBLEM IDENTIFIED	11
2.2 GAPS IDENTIFIED	15
2.3 RESEARCH OBJECTIVES	16
3 PROPOSED METHODOLOGY	17
3.1 ARCHITECTURAL DESIGN	17
3.2 MODULE SPLIT-UP	18
3.2.1 Traditional Deep Learning CNN	18
3.2.2 Tuned CNN	20

3.2.3	Hypercomplex-Valued CNN	23
3.2.4	Relapse Prediction Module	24
4	EXPERIMENTAL RESULTS	27
4.1	DATASET DESCRIPTION	27
4.1.1	MRI Images	27
4.1.2	Molecular Subtypes	28
4.1.3	Clinical Features	33
4.2	ECOSYSTEM	36
4.2.1	Hardware	36
4.2.2	Software	37
4.3	EXPERIMENTS CONDUCTED	39
4.3.1	Classification Model	39
4.3.2	Prediction model	39
5	PERFORMANCE ANALYSIS	41
5.1	TRADITIONAL DEEP LEARNING CNN	41
5.2	TUNED CNN MODEL	43
5.3	HYPERCOMPLEX VALUED CNN	45
5.3.1	Comparing the performance of Hyperparameter Tuned CNN with HyperComplex-Valued CNN	47
5.4	RELAPSE PREDICTION MODEL	47
6	SOCIAL IMPACT AND SUSTAINABILITY	50
6.1	APPLICATION IN SOCIETY, HEALTH AND ENVIRONMENTAL ISSUES	50
6.2	SUSTAINABILITY	51

7	CONCLUSIONS AND FUTURE WORK	52
7.1	FUTURE ENHANCEMENTS	52
	REFERENCES	53

LIST OF TABLES

1.1	Lifetime breast cancer risk	4
1.2	Survival Rates across Stages	8
3.1	The multiplication table of the eight algebras	24
4.1	Features of Clinical Data	35
5.1	Comparison report	47

LIST OF FIGURES

1.1	Breast Cancer with Age	4
1.2	Death rate over the years	5
3.1	The architectural model of the system	17
3.2	VGG 16 model for transfer learning	18
3.3	Figure depicting Transfer Learning	19
3.4	Figure depicting tuning of hyperparameters	20
3.5	Various configurations of learning rate	21
3.6	Image depicting SVM algorithm	25
3.7	Figure depicting grid search	26
4.1	MRI Images of the Molecular Subtypes of Breast Cancer	28
5.1	Graph depicting training and validation accuracy	41
5.2	Graph depicting training and validation loss	42
5.3	Results for the traditional CNN model	43
5.4	Graph depicting training and validation accuracy	43
5.5	Graph depicting training and validation loss	44
5.6	Classification report for the tuned CNN model	44
5.7	Graph depicting model accuracy	45
5.8	Graph depicting model loss	46
5.9	Classification report for the HvCNN model	46
5.10	Performance of the SVM model showing accuracies for different SVMs	47
5.11	ROC curve for svm model	48
5.12	Classification report for relapse model with GridSearchCV used to optimize hyperparameters for SVM model performance	48
5.13	ROC curve for optimised model using GridSearchCV	49

CHAPTER 1

INTRODUCTION

1.1 MOTIVATION

One of the most common malignant tumours in the world, breast cancer (BC) is responsible for 10.4% of all cancer-related deaths in women between the ages of 20 and 50. According to statistics from the World Health Organization, 2.3 million women received a BC diagnosis in 2020. BC is the most common cancer worldwide, with 7.8 million women receiving a diagnosis in the last five years. BC is the type of cancer that results in the greatest number of disability-adjusted life years (DALYs) for females worldwide. In every nation on the earth, breast cancer affects women after puberty at any age, with rates increasing as they get older. Due to all of these factors, a trustworthy and accurate system is constantly required in order to aid in the early identification and diagnosis of breast cancer diseases in order to decrease the number of fatalities. Early breast cancer discovery can lead to successful treatment. The initial separation of cancer cases from non-cancer cases involves the use of magnetic resonance imaging (MRI) pictures for the diagnosis of breast cancer. Due to the non-specific character of Breast Cancer symptoms and signs, misinterpretation happens frequently, making it difficult for laboratory users to properly examine these MRI pictures. Additionally, relapse prediction can significantly assist patients in maintaining awareness of their medical condition, survival statistics, and healthy lifestyle choices. Our system aims to overcome the difficulties faced while predicting BC

by providing an automated system to classify the MRI images into it's molecular sub-types which will aid the medical professionals in their diagnosis.

1.2 BACKGROUND

Breast cancer is a type of cancer that develops in the breast tissue. It can occur in both men and women, but it is more commonly diagnosed in women. Early breast cancer diagnosis is crucial since it considerably improves the likelihood of effective therapy and recovery. Early detection of breast cancer increases the likelihood that it will be small and limited to the breast tissue, making surgery and other therapies easier to perform. Breast lumps or thickenings, changes in breast size or form, nipple discharge or inversion, and skin changes on the breast, such as redness or dimpling, are all signs of breast cancer. But a lot of breast cancer cases don't show any signs, which is why routine screening is so crucial. Breast cancer can be detected using a variety of techniques, such as mammography, ultrasound, MRI, and biopsy. Women who are more likely to develop breast cancer, such as those with a family history of the disease, may have to start screening earlier or have screenings more frequently.

1.2.1 Factors Contributing to Breast Cancer

1.2.1.1 Lifestyle Factors

Research has shown that a variety of lifestyle factors may play a role in the development of breast cancer, just as they do with other types of cancer.

- **Weight:** According to recent research, being post-menopausal and overweight or obese increases the risk of developing breast cancer. Additionally, there is a greater chance of the cancer returning following treatment.
- **Physical Exercise:** Less physical activity is linked to a higher risk of breast cancer development and a higher likelihood of the disease returning after treatment.
- **Alcohol:** According to recent studies, drinking more than 1 to 2 drinks per day—including beer, wine, and spirits—increases the risk of developing breast cancer. Three to four servings of alcohol per week are the recommended upper limit.
- **Food:** There is no credible research to support the idea that consuming or abstaining from a particular food increases the risk of getting breast cancer or having it return after treatment. But there are other health advantages to eating more fruits and vegetables and less animal fat, including a modest reduction in the risk of breast cancer.

1.2.1.2 Age

Age raises the risk of developing breast cancer, with most cases (around 80%) occurring after age 50. The Figure 1.1 shows the age (in years) plotted against incidence per 100,000, from that we can see the average age at which breast cancer is diagnosed is 63.



FIGURE 1.1: Breast Cancer with Age

SOURCE: Slideshare, Breast Cancer by Asheer Khan

1.2.1.3 Genetic Risk Factor

A number of inherited genetic variants have been associated with an elevated risk of breast cancer as well as other cancers.

	Lifetime breast cancer risk	Median age of breast cancer onset (y)
General population	11%	61
<i>BRCA1</i>	65%	43
<i>BRCA2</i>	45%	41

TABLE 1.1: Lifetime breast cancer risk

SOURCE: Slideshare, Breast Cancer by Asheer Khan

Table 1.1 shows the most often identified genes associated with breast cancer - BRCA1 or BRCA2 and their lifetime breast cancer risk (in percentage) and the median age of each for breast cancer onset (in years).

1.2.1.4 Race and Ethnicity

Regardless of ethnicity, breast cancer is the most common cancer diagnosis in women, followed by skin cancer. Breast cancer is more common among Black women than White women over the age of 45, despite the fact that White women are more prone than Black women to have the disease. Also more likely to pass away from the illness are black women. Divergences in biology, other health issues, and socioeconomic variables that affect access to and utilisation of medical treatment are possible causes of survival discrepancies. Figure 1.2 shows the death rate over the years in different race and ethnicity

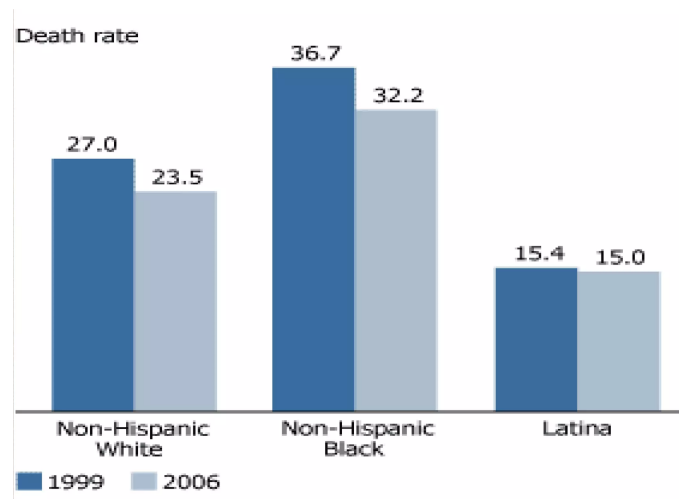


FIGURE 1.2: Death rate over the years

SOURCE: Slideshare, Breast Cancer by Asheer Khan

1.2.2 Staging of Breast Cancer

- **Stage 0:** A disease in stage zero (0) only affects the ducts of the breast tissue and has not progressed to the breast's surrounding tissue. It is also known as in situ cancer (Tis, N0, M0) or non-invasive cancer.
- **Stage I:**
 - Stage IA: It describes a tumour as being small, invasive, and not lymphocytic (T1, N0, M0).
 - Stage IB: Lymph nodes have been affected by the disease, and the cancer there is larger than 0.2 mm but less than 2 mm in size. Either there is no indication of a breast tumour or the breast tumour (T0 or T1, N1mi, M0) is 20 mm or smaller.
- **Stage II:**
 - Stage IIA: Any one of the following conditions
 - * The disease has expanded to one to three axillary lymph nodes but there is no sign of a tumour in the breast. T0, N1, and M0 are not remote sections of the body where it has spread.
 - * The tumour has progressed to one to three axillary lymph nodes (T1, N1, M0) and is 20 mm or less in size.
 - * The tumour has not migrated to the axillary lymph nodes (T2, N0, M0) and is greater than 20 mm but not 50 mm.
 - Stage IIB: One of the following circumstances:
 - * The tumour has migrated to one to three axillary lymph nodes (T2, N1, M0), and it is greater than 20 mm but not bigger than 50 mm.

- * The axillary lymph nodes (T3, N0, M0) have not yet been reached by the tumour, despite its size exceeding 50 mm.

- **Stage III:**

- Stage IIIA: The tumour, regardless of size, has metastasized to the internal mammary lymph nodes or to 4 to 9 axillary lymph nodes. The body's other organs (T0, T1, T2, or T3; N2; M0) have not been affected. Stage IIIA can also refer to a tumour that is 50 mm or greater and has reached one to three axillary lymph nodes (T3, N1, M0).
- Stage IIIB: The tumour has spread to the chest wall, resulted in breast edoema or ulceration, or inflammatory breast cancer has been identified. Up to 9 axillary or internal mammary lymph nodes may or may not have been affected by its dissemination. The T4; N0, N1, or N2; M0; other body regions have not been affected by it.
- Stage IIIC: Any tumour that has reached 10 or more axillary lymph nodes, internal mammary lymph nodes, or the lymph nodes under the collarbone is considered to be in stage IIIC. No T, N3, or M0 portions of the body have been affected by it.

- **Stage IV:** Any size tumour that has metastasized to the bones, lungs, brain, liver, distant lymph nodes, or chest wall (any T, any N, M1). About 6% of the time, metastatic cancer is discovered at the time of the initial cancer diagnosis. De novo metastatic breast cancer is one name for this. The majority of the time, metastatic breast cancer is discovered following an earlier diagnosis of early-stage breast cancer. Find out more about breast cancer that has spread.

- **Recurrent:** Recurrent cancer, which can be local, regional, or distant, is cancer that has returned after treatment. There will be more testing to determine the amount of the cancer recurrence if it does. These examinations and scans frequently resemble those carried out at the time of the first diagnosis.

Table 1.2 shows the 5-year relative survival rate across the stages.

Stage	5-year Relative Survival Rate
0	100%
I	100%
II	93%
III	72%
IV	22%

TABLE 1.2: Survival Rates across Stages

SOURCE: Slideshare, Breast Cancer by Asheer Khan

1.3 PROBLEM DEFINITION

Following are the objectives of our proposed system:

- To provide an optimized solution to classify Breast Cancer into its molecular subtypes - Luminal, ER/PR positive and HER2 Positive, HER2, Triple negative using traditional DL CNN, Tuned CNN by using a Pytorch Gradient Calculation framework for tuning a subset of CNN hyperparameters and Hypercomplex-Valued CNN by using hypercomplex algebras to reduce the number of parameters used in traditional CNN significantly.
- To perform a comparative analysis of the three different CNN models.
- To predict the relapse of Breast Cancer by using Tuned SVM using GridSearchCV.

1.4 ORGANIZATION OF THE REPORT

The report is organized as follows. The next chapter, Chapter 2, includes the literature survey done on papers related to the work, the research gap identified and the research objectives of the project. Chapter 3 elaborates on the proposed methodology and architecture for the system with each section highlighting a module. Chapter 4 describes the experimental results which includes the description of the dataset, the ecosystem and the experiments that were conducted. Chapter 5 includes a performance analysis of the different models.

Chapter 6 talks about the social impact and sustainability of the project. In chapter 7, we end with a conclusion and the suggestions for future work. Chapter 8 lists out the references used in the project.

CHAPTER 2

LITERATURE SURVEY

2.1 PAPERS RELATED TO THE PROBLEM IDENTIFIED

Ahmad LG et al. [1] investigated three classification models, DT, SVM, and ANN, and found that SVM had the highest accuracy when used to create models to predict the recurrence of breast cancer.

Danish Vasan et al. [2] proposed the IMCFN (Image-based Malware Classification using Fine-tuned Convolutional Neural Network Architecture) classifier to identify variations of malware families and improve malware detection using CNN-based deep learning architecture. The unprocessed malware binaries are converted into coloured images using a method for multiclass classification issues that allows the optimised CNN architecture to use them to locate and categorise malware families.

Eva Tuba et. al [3] put forth a simple bare bones firework approach for fine-tuning a selection of CNN hyperparameters. On a common benchmark dataset for the detection of acute lymphoblastic leukaemia, the proposed technique was evaluated. It was compared to CNN without hyperparameter tuning and the optimised SVM method, and it outperformed the other two techniques in terms of accuracy.

Guilherme Vieira et al.[4] combined real-valued convolutional networks with eight hypercomplex-valued convolutional neural networks (HvCNNs) to perform

the classification job. The outcomes demonstrated that HvCNNs outperform the real-valued model, displaying superior accuracy with a significantly fewer number of parameters.

Jesse C. Sealand et. al [5] proposed a study that utilised four machine learning gradient-boosting algorithms and five tree-based models to find patterns in ALL patients who experience relapses and use those patterns to predict relapses in advance.

J. Marget et al. [6] suggested a convolutional neural network-based technique to anticipate the five most typical heart views and automatically extract missing or noisy cardiac acquisition plane information from magnetic resonance imaging. The convolutional neural network (CNN) was initially trained on a sizable dataset for natural image identification (Imagenet ILSVRC2012) then fine-tuned before applying the learned feature representations to the recognition of cardiac views.

Jose M. Jerez-Aragones et al. [7] suggested a decision support tool for prediction of breast cancer recurrence that combines an innovative algorithm, TDIDT (control of induction by sample division method, CIDIM), to choose the most important prognostic factors for their precise prognosis of breast cancer, with a system composed of various neural network topologies that takes the selected variables as input in order to reach good correct classification probability.

Mandeep Rana et al. [8] proposed a study to determine if breast cancer is benign or malignant and to forecast the recurrence and non-recurrence of malignant cases after a specific time period. Support Vector Machine (SVM) was shown to be the most suitable for predictive analysis, and KNN outperformed Naive Bayes for the

overall methodology. They have employed machine learning techniques such as Logistic Regression, Support Vector Machine, KNN, and Naive Bayes.

Marcos Eduardo Valle et al. [9] extended the bipolar RCNNs to handle hypercomplex-valued input. The stability of the novel hypercomplex-valued RCNNs employing synchronous and asynchronous update modes is then addressed after the mathematical foundation for a large class of hypercomplex-valued RCNNs is presented. The computational tests validate the potential use of hypercomplex-valued RCNNs as associative memories aimed at the storage and retrieval of grayscale images.

Mustafa Ghaderzadeh et al. [10] utilised a model based on deep convolutional neural networks to distinguish ALL instances from hematogone cases and then identify ALL subtypes. Ten well-known CNN architectures (EfficientNet, MobileNetV3, VGG-19, Xception, InceptionV3, ResNet50V2, VGG-16, NASNetLarge, InceptionResNetV2, and DenseNet201) were used for feature extraction of various data classes after colour thresholding-based segmentation in the HSV colour space by designing a two-channel network. Based on DenseNet201, a model was created and put forth that performed the best.

Richard Ha et al. [11] devised a system to identify the molecular subtype of a breast cancer based on MRI characteristics. Initially, 3D segmentation using a 3D slicer was performed on post-contrast MRI images. A 14-layer CNN architecture was created. In the early tiers, residual connections were utilised. Deeper in the network, Inception-style layers were used, along with significant regularisation that included dropout, L2, feature map dropout, and transition layers.

Srikanth Tammina [12] classified images using one of the pre-trained models, VGG-16 with Deep Convolutional Neural Network. In order to transfer low-level characteristics, such as edges, corners, and rotation, and learn new level features related to the goal problem, which is to categorise the images, the pretrained VGG-16 model is utilised as leverage.

Sungmin Rhee et al. [13] used graph CNN to learn the expression patterns of cooperative gene communities, and RN is used to understand the relationships between the learnt patterns. The PAM50 breast cancer subtype classification task, the industry-standard classification of breast cancer subtypes with clinical relevance, is used to test the proposed model.

Tianwen Xie et al. [14] put out an innovative two-stage feature selection strategy combining conventional statistics and machine learning-based techniques. The reliability of the 4-IHC classification and the distinction between triple negative (TN) and non-TN tumours were evaluated.

Xiaoli Li et al. [15] proposed a system to construct a computer-aided diagnostic (CAD) system for classifying breast cancer molecular subtypes using deep learning characteristics. A pre-trained convolutional neural network (CNN) was utilised by the scientists to extract deep learning features from a dataset of breast cancer histopathology images. After that, a support vector machine (SVM) classifier was used to identify the molecular subtype of the breast cancer using these features. The findings demonstrated that the suggested CAD method, with an overall accuracy of 92.16 %, was very accurate in categorising breast cancer molecular subtypes.

Yang Zhang et al. [16] proposed a system that used the smallest bounding box covering the tumour ROI as the input for deep learning to develop the model in the training dataset with the help of a conventional CNN, convolutional long short term memory (CLSTM), and transfer learning. CNN and CLSTM both had higher mean accuracy when tested using 10-fold cross-validation.

Zhencun Jiang et al. [17] introduced the ViT-CNN ensemble model to aid in the diagnosis of acute lymphoblastic leukaemia by identifying cancer cells images and normal cells images. The vision transformer and convolutional neural network (CNN) models are combined to create the ViT-CNN ensemble model. The findings demonstrated that the model suggested in this article was more accurate than other models and had a balanced capacity for classification.

2.2 GAPS IDENTIFIED

While there have been earlier studies on classifying breast cancer into its subtypes based on MRI images using CNN, this research uses a novel approach by comparing three different CNN models - the traditional deep learning CNN model, the tuned CNN model and the hypercomplex-valued CNN model which has been extended from a binary classification model to a multi-classification model and hasn't been used before to classify breast cancer. Overall, it appears that this study makes a significant contribution to the classification of breast cancer into its molecular subtypes and fills in significant research gaps by offering a more accurate method of classification,

2.3 RESEARCH OBJECTIVES

In this research, a convolutional neural network (CNN) is proposed for classifying MRI scans of breasts. To achieve better results, it is necessary to tune CNN hyperparameters which is an NP-hard optimization problem. In this paper, the Pytorch Gradient Calculation framework is adjusted for tuning some of the CNN hyperparameters. On the other hand, Hypercomplex-Valued CNN (HvCNN), based on Clifford algebra processing of HSV-encoded images is used to classify breast cancer into its molecular subtypes. The HvCNN is known to have a much simpler architecture with significantly fewer parameters than real valued CNN. Hence performance of the two techniques is compared with traditional DL CNN and results are inferred. The survivors of breast cancer are still at risk for relapse after remission, and once the disease relapses, the survival rate is much lower. Data mining and analysis can be used to identify patterns in those patients who experience a relapse. By analysing data of known relapses, it could be possible to identify the factors surrounding the relapse and make a positive impact on the survivability of people who do relapse. A thorough analysis of data can potentially identify risk factors and reduce the risk of relapse in the first place. Hence, an SVM (Support Vector Machine) module with GridSearchCV for hyperparameter tuning is proposed for predicting relapse in a patient based on their history and other details.

CHAPTER 3

PROPOSED METHODOLOGY

3.1 ARCHITECTURAL DESIGN

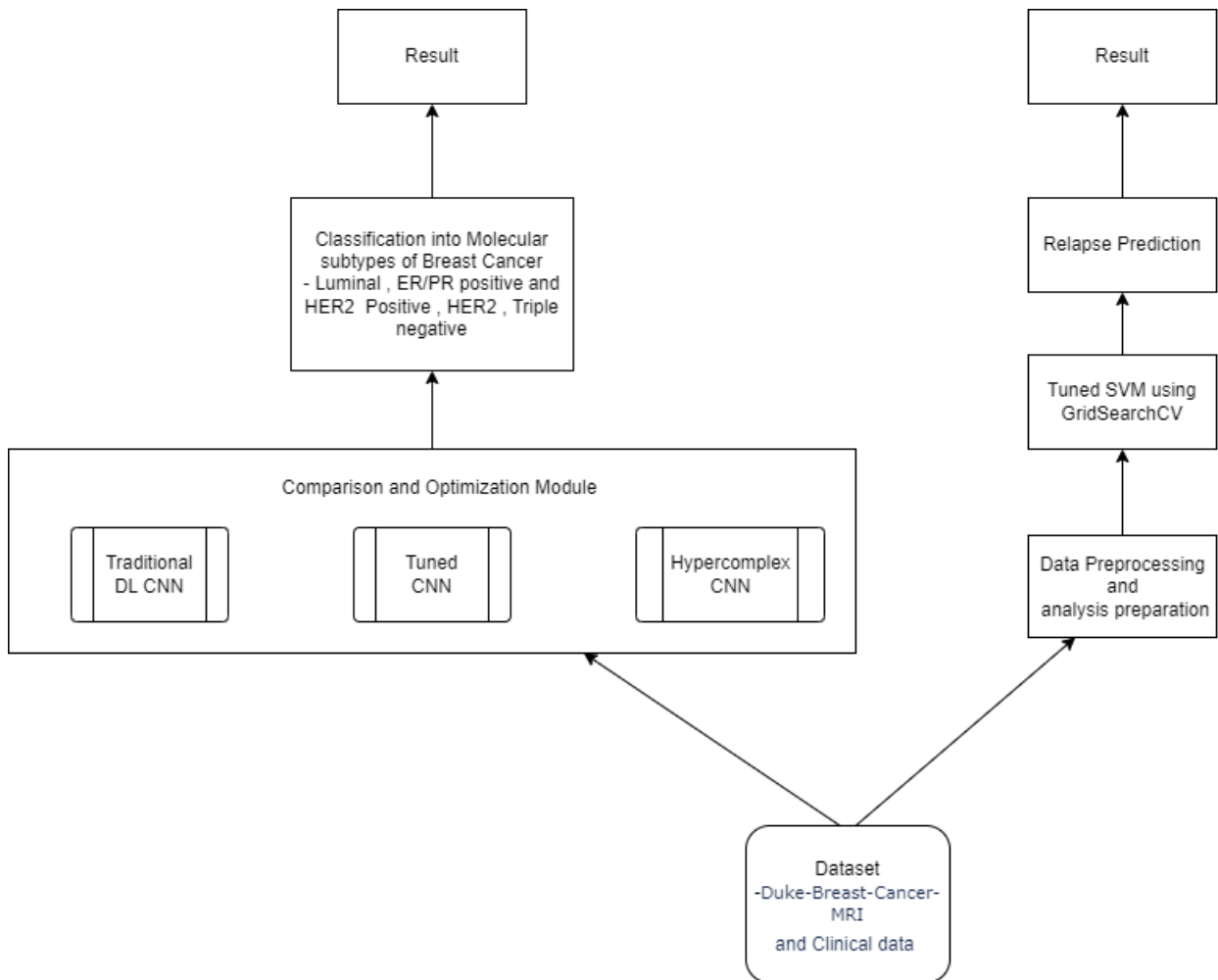


FIGURE 3.1: The architectural model of the system

From figure 3.1 we can see the flow of the system is as follows : The dataset consists of patient's MRI images and their clinical data . The MRI images are sent to a classification model which consists of 3 different CNN models which

are compared and the best CNN model is taken to classify the mri images into molecular subtypes. The clinical data is preprocessed and then passed to a tuned svm model using GridSearchCV which is used to predict whether the cancer will relapse.

3.2 MODULE SPLIT-UP

3.2.1 Traditional Deep Learning CNN

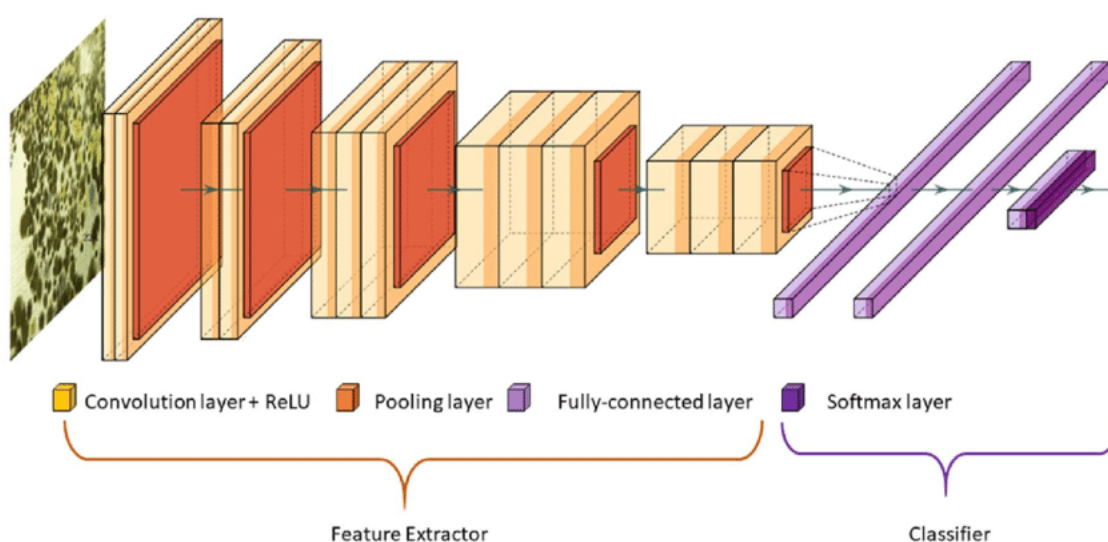


FIGURE 3.2: VGG 16 model for transfer learning

SOURCE: ResearchGate, Deep Learning for Detecting Building Defects Using Convolutional Neural Networks

Convolutional, pooling, and fully connected layers constitute the layers that make up the conventional deep learning Convolutional Neural Network (CNN) model. Learning hierarchical representations of the breast cancer MRI images is the aim of these layers. This model uses transfer learning using vgg16. Architecture of vgg16 is depicted in figure 3.2.

In transfer learning, the CNNs combine convolution layers with filters to assist them identify the key elements in an image. These character traits help identify a certain image. All these properties are internal learning that occurs whenever a CNN is trained on a large collection of images. Additionally, the amount of parameters, also known as weights, that are learned when using a deep CNN can reach millions. Therefore, it takes time when several factors need to be mastered. Transfer learning can be helpful here.

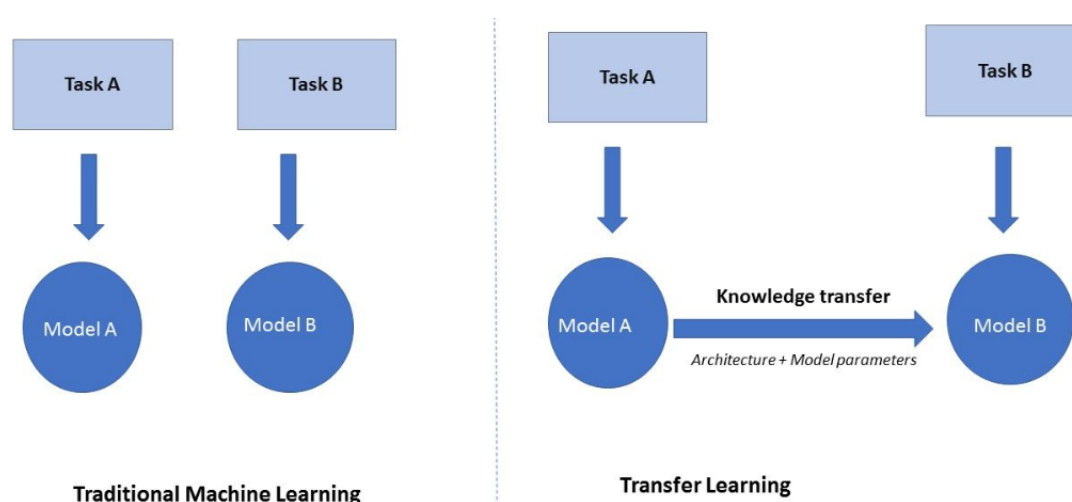


FIGURE 3.3: Figure depicting Transfer Learning

SOURCE: Packtpub, Big Data and Business Intelligence, Introduction to Transfer learning

As shown in figure 3.3, Transfer learning is a strategy where we take a model that has been trained for one machine learning task and use it as the foundation for another. This method is used in a number of deep learning fields, including image classification and natural language processing. By using transfer learning in our model, bottleneck features are obtained to classify the images into their molecular subtypes.

3.2.2 Tuned CNN

Tuned CNNs are CNN models that have several hyperparameters adjusted specifically for a given task or dataset. As shown in figure 3.4, Hyper-parameters are configurations that the user selects rather than learning through training. The model's performance is maximised by using that set of hyperparameters, which minimises a predetermined loss function and resulting in better results with fewer errors. It should be noted that the learning algorithm attempts to discover the best solution within the constraints and optimises the loss depending on the input data. Hyperparameters, however, precisely specify this configuration.

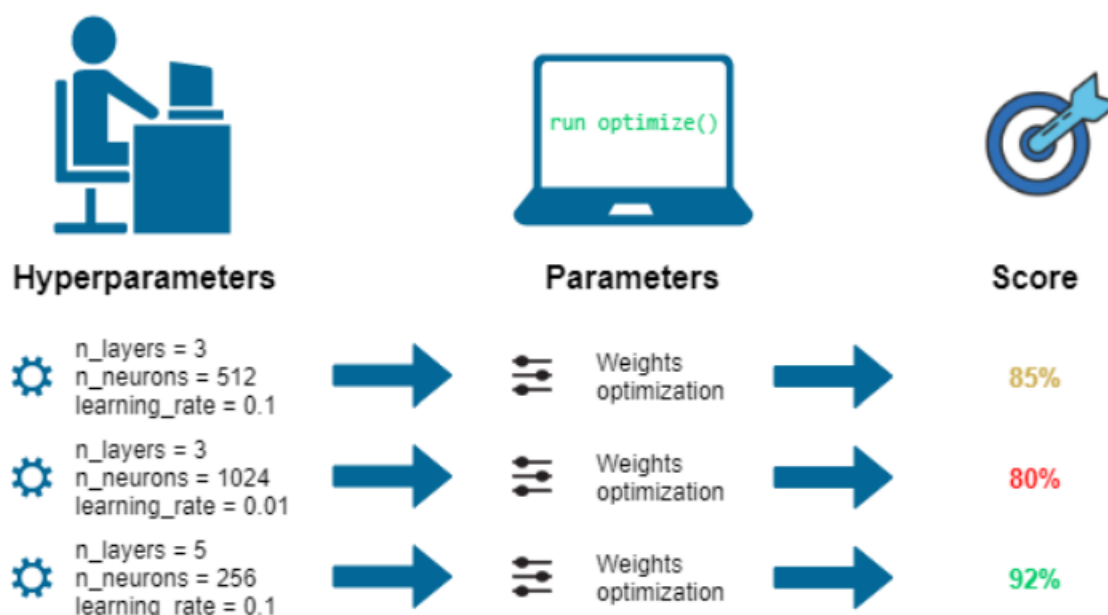


FIGURE 3.4: Figure depicting tuning of hyperparameters

SOURCE: KDnuggets, Practical hyperparameter optimization

Hyperparameters explored in our System for tuned CNN:

- **Learning Rate:** Learning rate describes how our network's weights are adjusted in relation to loss gradient descent. The most crucial hyper-parameter for fine-tuning neural networks is the learning rate. A model's ability to learn could mean the difference between one that doesn't advance and one that produces cutting-edge outcomes.

Figure 3.5 illustrates the various configurations that can occur when setting the learning rate.

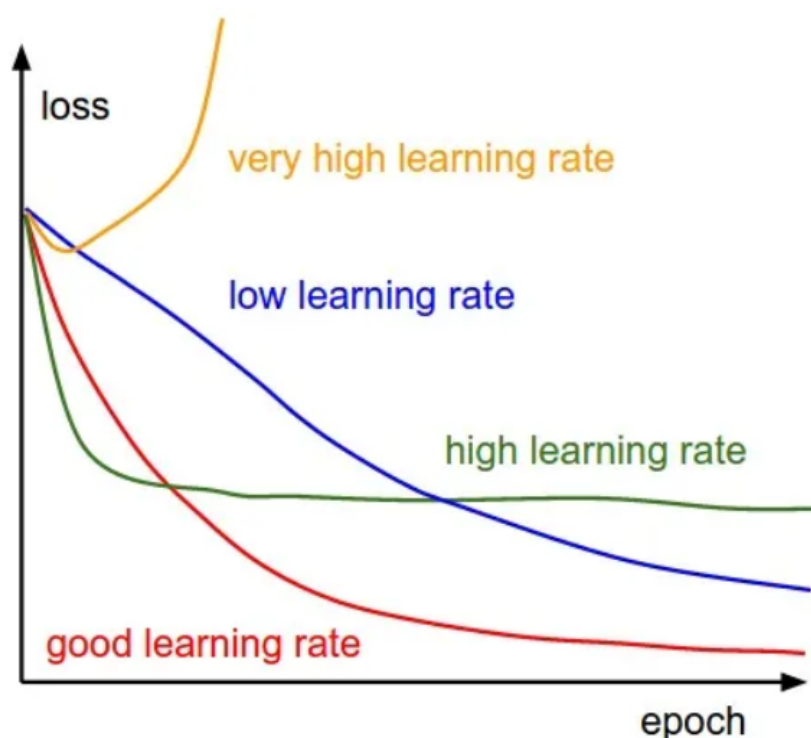


FIGURE 3.5: Various configurations of learning rate

SOURCE: Towards Data Science, Understanding Learning Rate

- **Dropout Rate:** The chance of training a specific node in a layer is the default meaning of the dropout hyperparameter, where 1.0 denotes no dropout and

0.0 denotes no outputs from the layer. Between 0.5 and 0.8 is an acceptable range for dropout in a hidden layer. The dropout rate for input layers is higher, typically 0.8.

- **Batch Size:** The batch size is a hyperparameter that specifies how many samples must be processed before the internal model parameters are updated.
- **Hidden units:** The intermediary neurons or processing units that are not immediately visible from the network's input or output are referred to as hidden units in a convolutional neural network (CNN). Feature maps are another name for these concealed units.

Each convolutional layer in a CNN applies a different set of filters to the input image in order to extract important characteristics. Each convolutional layer produces a set of feature maps, each of which corresponds to a different filter that was applied to the input. The number of filters used in each convolutional layer determines how many hidden units are present in a CNN. A hidden unit in the following layer is matched to each filter in the convolutional layer. Thus, the depth and architecture of the network can affect the number of hidden units in a CNN. The weights and biases of the filters used in the convolutional layers determine how these hidden units are activated. The final layer's hidden units' activation levels are then utilised to make predictions or categorise the input image.

A pre-trained VGG-16 model serves as the transfer learning model. When the transfer learning model is loaded, the initial classifier layers are swapped out for new ones for the improved model, and the model weights are locked to prevent

further training. During training, only the weights of the newest neural network layers are modified. In order to facilitate the exploration, the model parameters are defined as a set. Finally, after fine-tuning the hyperparameters, the pictures are classified into their molecular subtypes using the CNN model with the best hyperparameter values.

3.2.3 Hypercomplex-Valued CNN

Eight hypercomplex-valued convolutional neural networks (HvCNNs) are used for the categorization. Hv-CNNs can be used to analyze the images to classify Breast Cancer. Hypercomplex numbers provide a natural representation of orientation and rotation information, which can be useful for analyzing the structural and geometric features of breast cells in images. The input image would be represented as a hypercomplex-valued data tensor, and the convolutional layer performs convolution operations on the input data using hypercomplex-valued filters. The features extracted by the convolutional layer is then processed by fully connected layers, which will make the final classification decisions based on the learned features. The hypercomplex-valued model has a layer layout of convolutional layers followed by a max pooling layer with kernels, where each channel of the hypercomplex-valued corresponds to four real-valued feature channels, so that it uses much fewer filters per convolution layer.

A quaternion numerical network constructed using quaternion algebra is used. Quaternions are the four-dimensional extension of complex numbers.

$A[-1, -1]$, $A[-1, +1]$, $A[+1, -1]$, and $A[+1, +1]$

$B[-1, -1]$, $B[-1, +1]$, $B[+1, -1]$, $B[+1, +1]$

There are a total of eight 4-dimensional hypercomplex algebras. They are all associative, four anti-commutative and the rest commutative.

	i	j	k
i	s_{11}	$s_{12}k$	$s_{13}j$
j	$s_{21}k$	s_{22}	$s_{23}i$
k	$s_{31}j$	$s_{32}i$	s_{33}

TABLE 3.1: The multiplication table of the eight algebras

3.2.4 Relapse Prediction Module

Support Vector Machine (SVM), a component of the Scikit Learn package, is the algorithm employed. Support vector machines (SVMs), one of the most popular supervised learning techniques, are frequently used to solve machine learning regression problems. The goal of the SVM algorithm is to define an ideal boundary or decision line that can classify the n-dimensional space, making it straightforward to assign new data points to the proper category in the future. The optimal hyperplane shown in figure 3.6 is the best-case decision boundary.

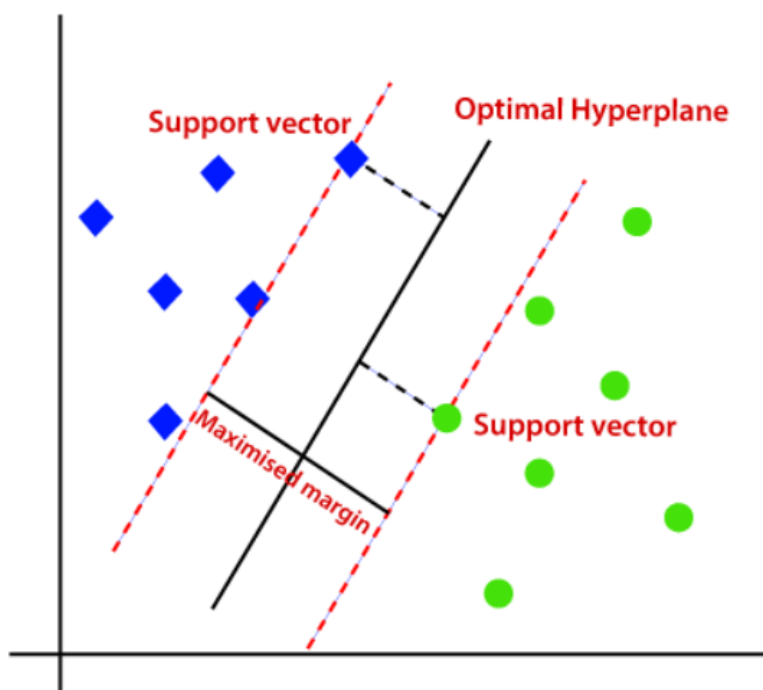


FIGURE 3.6: Image depicting SVM algorithm

SOURCE: Analytics Vidhya, SVM

For fine-tuning the hyperparameters, we use GridSearchCV. By determining the ideal combination of hyperparameters, the hyperparameter tuning technique known as GridSearchCV is used to improve the performance of a model. As shown in figure 3.7, a grid of all possible combinations is created and explored to optimise set of hyperparameters.

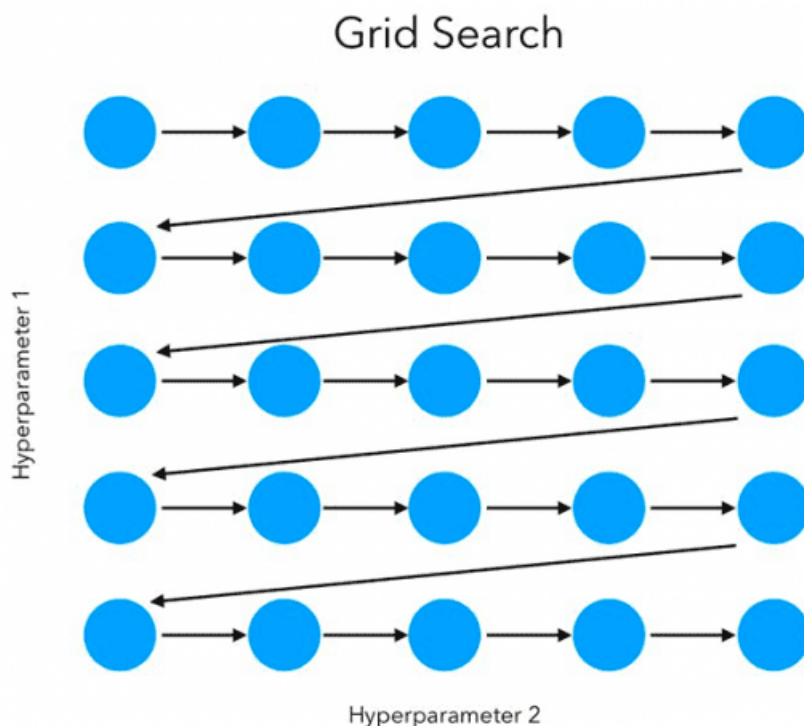


FIGURE 3.7: Figure depicting grid search

SOURCE: Github, Mael Fabien, Grid Search

The model is then trained with each conceivable combination of hyperparameters, and the performance of each combination is assessed using cross-validation. By dividing the data into training and validation sets, training the model on the training set, then assessing it on the validation set, cross-validation is a technique used to evaluate the generalisation performance of a model. The optimal values for hyperparameters cannot be determined in advance, thus we need consider all possible values before choosing the best ones. As manual tuning could need a lot of time and resources, we use GridSearchCV to automate the process.

CHAPTER 4

EXPERIMENTAL RESULTS

4.1 DATASET DESCRIPTION

The breast MRI dataset includes 922 patients with invasive breast cancer who were treated at Duke Hospital between 1 January 2000 and 23 March 2014 and who had access to pre-operative MRI at Duke Hospital. The dataset consists of MRI scans of 992 patients and their clinical data.

4.1.1 MRI Images

Following are the MRI scans of 4 different patients belonging to different molecular subtypes namely:

- Luminal-like
- ER/PR Positive, HER2 Positive
- HER2
- Triple Negative

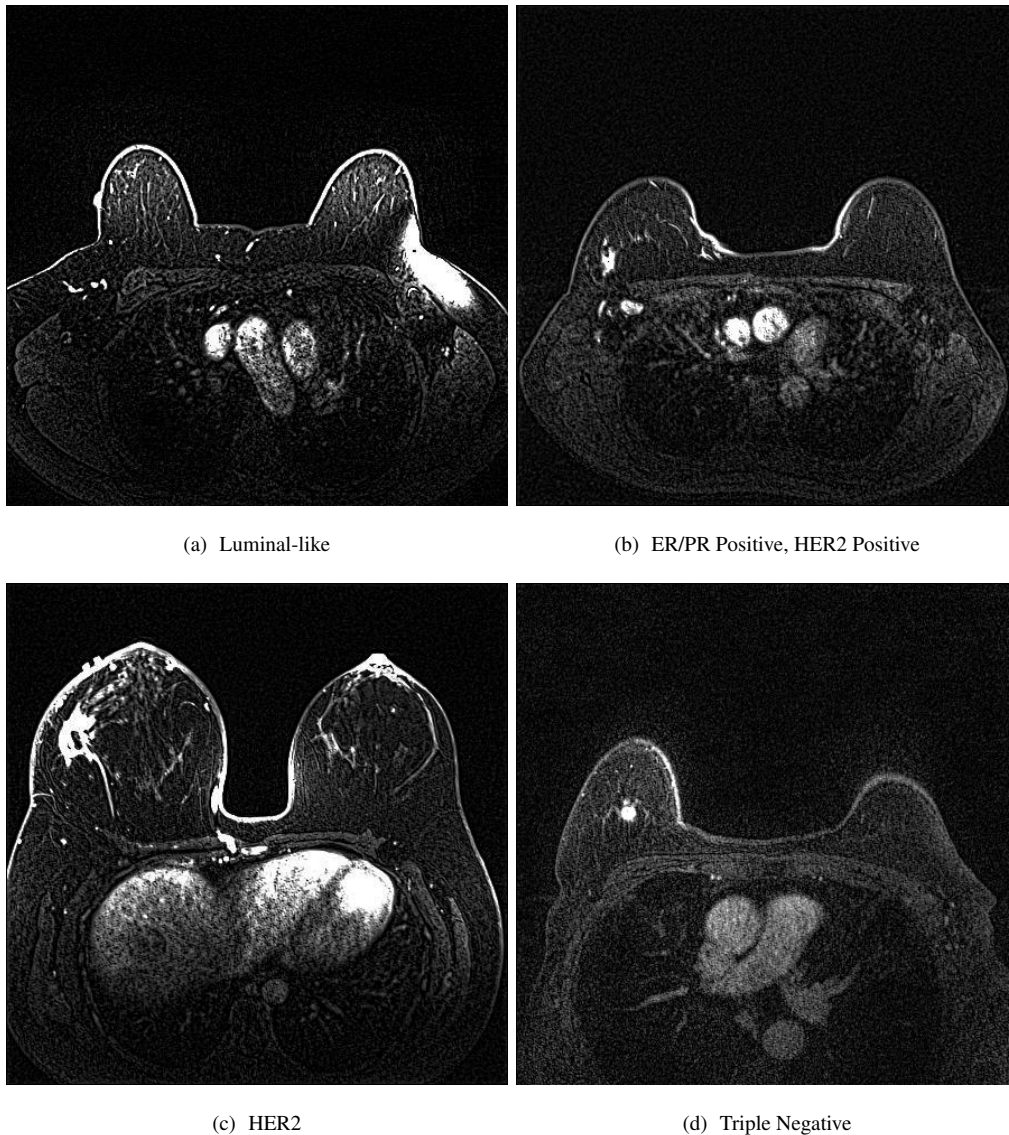


FIGURE 4.1: MRI Images of the Molecular Subtypes of Breast Cancer

4.1.2 Molecular Subtypes

4.1.2.1 Luminal-like

The figure 4.1 (a) shows a luminal-like tumour. The presence of ER and/or PR, the absence of HER2, and low expression of the cell proliferation marker Ki-67 (less than 20%) are the characteristics of luminal A tumours. Clinically, they have the greatest prognosis due to their low grade, moderate growth, lower relapse

incidence, and higher survival rate. These cancers have a high rate of response to hormone therapy (tamoxifen or aromatase inhibitors), but chemotherapy has a less impact. To determine which patients would benefit from adjuvant chemotherapy treatment based on the risk of relapse and survival rate, the use of genetic platforms is advised in this group, according to the European Society for Medical Oncology (ESMO) and National Comprehensive Cancer Network from USA (NCCN) Guidelines. Relapses are more common at the bone level and less common in the visceral and central nervous systems (CNS). In the event of a relapse, they also had a longer survival time. When compared to Luminal A tumours, Luminal B tumours have a higher grade and a worse prognosis. They exhibit a high expression of Ki67 (more than 20%), are ER positive, and may be PR negative. They typically have a high or intermediate histologic grade. Hormonal therapy may help these tumours together with chemotherapy. They have a worse prognosis and proliferate more quickly than luminal A due to the increased Ki67 (32). 10% to 20% of luminal tumours are made up of it. It expresses cell cycle and proliferation genes more highly than oestrogen receptors, which are expressed at a moderately modest level. It stands for the subset of luminal tumours that has the worst outlook. In comparison to the prior group, they benefit more from chemotherapy and hormone therapy. Although visceral recurrence is more common than bone recurrence, they also have a worse rate of survival from diagnosis to relapse.

4.1.2.2 ER/PR Positive

The figure 4.1 (b) shows a ER/PR Positive, HER2 Positive tumour. When the cancer cells have receptors for the chemicals progesterone and oestrogen on their

surface, it is known as ER/PR positive breast cancer. As they enable the cancer cells to proliferate and multiply in response to the presence of these hormones, these receptors play a vital role in the onset and progression of the disease. The protein Ki-67, which is involved in cell growth, is one such marker. Compared to tumours with low levels of Ki-67, those with high levels are more likely to be aggressive and have a worse prognosis. HER2, a protein that is over expressed in some breast cancers, is another marker that is frequently employed in the classification of ER/PR positive breast cancer. HER2 positive tumours may need targeted medicines like Herceptin in addition to conventional therapies like chemotherapy. The molecular characterisation of ER/PR positive breast cancer is likewise becoming more and more dependent on genomic profiling. Hormone receptors are present, however ER/PR positive breast cancer also has specific molecular characteristics. For instance, these tumours frequently have a lower tumour grade, which denotes that they are generally less aggressive and more unlikely to metastasize.

4.1.2.3 HER2 Positive

About 10-15% of breast tumours are HER2-positive, which are distinguished by strong HER2 expression and the absence of ER and PR. They develop more quickly than luminal ones, and since HER2-targeted medicines were developed, the outlook has improved. The subtype that is HER2-positive is more aggressive and rapidly expanding. HER2-enriched (HER2+, E-, PR-, Ki-67:30%) and luminal HER2 (E+, PR+, HER2+, and Ki-67:15-30%) are two subgroups within this that can be identified. They require specific drugs that target the HER2/neu protein, such as trastuzumab, trastuzumab combined with emtasin (T-DM1),

pertuzumab, and tyrosine kinase inhibitors like lapatinib and neratinib, among others, in addition to surgery and treatment with targeted chemotherapy. They have a worse prognosis than luminal tumours. Chemotherapy treatments have a high rate of success with them. The most typical site for disseminated disease is the bone, and visceral relapses are more likely in this cohort than in the first group.

4.1.2.4 HER2 Negative

The figure 4.1 (c) shows a HER2 tumour. Human epidermal growth factor receptor 2 (HER2) is a protein that is present on the surface of breast cells. Breast cancer that is HER2 positive has an excess of this protein. On the other hand, HER2 negative breast cancer is a subtype of breast cancer in which the cancer cells do not over express the HER2 protein. A lump in the breast or armpit, nipple discharge, and changes in the breast's size or form can all be signs of HER2 negative breast cancer. It's crucial to remember that not all breast lumps are malignant and that other diseases like cysts or benign tumours can produce symptoms that are similar to those of cancer. The importance of having any unusual changes in the breast examined by a medical practitioner can not be overstated. Depending on the stage and severity of the cancer, HER2 negative breast cancer is often treated with a combination of surgery, radiation therapy, and chemotherapy. Some HER2 negative breast cancers that are ER positive (positive for the oestrogen receptor) may also benefit from hormone therapy.

4.1.2.5 Triple negative

The figure 4.1 (d) shows a Triple Negative tumor. Triple-negative breast cancer is ER-negative, PR-negative, and HER2-negative. They account for 20% of all breast cancer cases. Black women and those under the age of 40 are more likely to experience it. The TNBC subtype is further divided into many subgroups, the most common of which are basal-like (BL1 and BL2), claudin-low, mesenchymal (MES), luminal androgen receptor (LAR), and immunomodulatory (IM). The first two categories account for between 50 and 70 percent and 20 to 30 percent of cases, respectively, of the TNBC subtype. The clinical outcomes, phenotypes, and pharmacological sensitivities of each of these are also distinctive. TNBC exhibits aggressive behaviour, and tumours that express the tumour suppressor genes BRCA1 and BRCA2 make up 80% of breast cancer tumours. Genetics, race, age, overweight and obesity, breastfeeding habits, and parity all affect a person's likelihood of getting TNBC. Aggressiveness, early relapse, and an increased propensity to present in an advanced stage are characteristics of TNBC. It has a rapid rate of proliferation, changes in DNA repair genes, and elevated genomic instability. Histologically, it is a heterogeneous tumour with subgroups that have varying prognoses that is poorly differentiated, highly proliferative, and heterogeneous. Based on immunohistochemical analysis, they can be separated into basal and non-basal TNBC; the former is distinguished from the latter by the expression of cytokeratins (CK)5/6 and the human epidermal growth factor receptor type 1 (EGFR1).

4.1.3 Clinical Features

Date of Birth (Days)	<= 26000 days
Menopause (at diagnosis)	0 = Pre, 1=Post
Metastatic at Presentation (Outside of Lymph Nodes)	0 = No, 1=Yes
ER	0 = Neg, 1=Pos
PR	0 = Neg, 1=Pos
HER2	0 = Neg, 1=Pos, 2 = Borderline
Mol Subtype	0 = luminal-like, 1 = ER/PR pos, HER2 pos, 2 = her2, 3 = trip neg
Oncotype score	<40
Staging(Tumor Size)# [T]	1-4
Staging(Nodes) #(Nx replaced by -1)[N]	1-4
Staging(Metastasis)#(Mx -replaced by -1)[M]	0, -1
Tumor Grade(T) (Tubule)	1=low 2=intermediate 3=high
Tumor Grade(N) (Nuclear)	1=low 2=intermediate 3=high
Tumor Grade(M)(Mitotic)	1=low 2=intermediate 3=high
Nottingham grade	1=low 2=intermediate 3=high
Histologic type	0=DCIS 1=ductal 2=lobular 3=metaplastic 4=LCIS 5=tubular 6=mixed 7=micropapillary 8=colloid 9=mucinous 10=medullary
Tumor Location	Side of cancer L=left R=right
Position	every bx positive for invasive
Bilateral Information	0 = No , 1=Yes
Multicentric/Multifocal	0 = No, 1=Yes
Contralateral Breast Involvement	0 = No, 1=Yes
Lymphadenopathy or Suspicious Nodes	0 = No, 1=Yes
Skin/Nipple Involvement	0 = No, 1=Yes
Pec/Chest Involvement	0 = No, 1=Yes
Surgery	0 = No, 1=Yes
Days to Surgery (from the date of diagnosis)	<200
Definitive Surgery Type	{0=BCS, 1=mastectomy}
Neoadjuvant Radiation Therapy	0 = No , 1=Yes
Adjuvant Radiation Therapy	0 = No, 1=Yes
Clinical Response, Evaluated Through Imaging	1=complete response on imaging, 2=not complete response, 3=imaging to assess treatment response is unavailable, NA=no neoadjuvant therapy or not enough information to assess neoadjuvant therapy status
Pathologic Response to Neoadjuvant Therapy	1=complete response on imaging, 2=not complete response, 3=imaging to assess treatment response is unavailable, NA=no neoadjuvant therapy or not

	enough information to assess neoadjuvant therapy status
Recurrence event	0 = No, 1=Yes
Days to local recurrence (from the date of diagnosis)	<2000
Days to distant recurrence(from the date of diagnosis)	<2000
Days to death (from the date of diagnosis)	<2000
Days to last local recurrence free assessment (from the date of diagnosis)	<3500
Days to last distant recurrence free <u>assessment</u> (from the date of diagnosis)	<3500
Age at last contact in EMR f/u(days)(from the date of diagnosis) , last time patient known to be alive, unless age of death is reported(in such case the age of death	<3500
Tumor Size (cm)	0-5
Neoadjuvant Chemotherapy	0 = No, 1=Yes
Adjuvant Chemotherapy	0 = No, 1=Yes
Neoadjuvant Endocrine Therapy Medications	0 = No, 1=Yes
Adjuvant Endocrine Therapy Medications	0 = No, 1=Yes
Known Ovarian Status	0 = No, 1=Yes
Number of Ovaries <u>In Situ</u>	0 = no ovaries intact, 1 = 1 ovary intact, 2 = 2 ovaries intact, NP = not pertinent to case
Therapeutic or Prophylactic Oophorectomy as part of Endocrine Therapy	0 = No, 1=Yes
Neoadjuvant Anti-Her2 Neu Therapy	0 = No, 1=Yes
Adjuvant Anti-Her2 Neu Therapy	0 = No, 1=Yes
Received Neoadjuvant Therapy or Not	0 = No, 1=Yes
Pathologic response to Neoadjuvant therapy: Pathologic stage (T) following neoadjuvant therapy	-1 = TX; 0 = T0; 1 = T1; 2 = T2; 3 = T3; 4 = T4; 5 = Tis (DCIS); NA = not applicable
Pathologic response to Neoadjuvant therapy: Pathologic stage (N) following neoadjuvant therapy	-1 = NX; 0 = N0; 1 = N1; 2 = N2; 3 = N3; NA = not applicable
Pathologic response to Neoadjuvant therapy: Pathologic stage (M) following neoadjuvant therapy	-1 = MX; 0 = M0; 1 = M1; NA = not applicable
Overall Near-complete Response: Stricter Definition	2 = Near complete (pathology report noted results constituted near-complete response to NAT) 3 = No residual disease, only atypical ductal hyperplasia 4 = No invasive carcinoma, DCIS only 5 = No invasive carcinoma, LCIS only 6 = 90% reduction in tumor volume 7 = 95% reduction

<p>Overall Near-complete Response: Looser Definition</p>	<p>18 = 99% of tumor obliterated but extensive residual DCIS</p> <p>2 = Near complete (pathology report noted results constituted near-complete response to NAT)</p> <p>3 = No residual disease, only atypical ductal hyperplasia</p> <p>4 = No invasive carcinoma, DCIS only</p> <p>5 = No invasive carcinoma, LCIS only</p> <p>6 = 90% reduction in tumor volume</p> <p>7 = 95% reduction</p> <p>8 = Near complete but DCIS</p> <p>9 = 90% reduction with DCIS present</p> <p>10 = No invasive disease but lymph nodes positive</p> <p>11 = No residual disease, but positive LNs and DCIS</p> <p>12 = Near complete response noted on path report, but positive LNs</p> <p>13 = 98% reduction with positive LNs</p> <p>14 = 95% fibrosis but positive lymph nodes</p> <p>15 = 90% reduction with positive LNs</p> <p>16 = > 95% <u>reduction</u> with only mucinous pools remaining</p> <p>17 = 1mm residual invasive but extensive DCIS</p> <p>18 = 99% of tumor obliterated but extensive residual DCIS</p>
<p>Near-complete Response (Graded Measure)</p>	<p>3 = No residual disease, only atypical ductal hyperplasia;</p> <p>4 = No invasive carcinoma, DCIS only; 5 = No invasive carcinoma, LCIS only; 6 = 90% reduction in tumor volume; 7 = 95% reduction; 8 = Near complete but DCIS; 9 = 90% reduction with DCIS present; 10 = No invasive disease but lymph nodes positive; 11 = No residual disease, but positive LNs and DCIS; 12 = Near complete response noted on path report, but positive LNs; 13 = 98% reduction with positive</p>

TABLE 4.1: Features of Clinical Data

The table 4.1 shows the 56 features present in the clinical data of 922 patients and their composition.

4.2 ECOSYSTEM

4.2.1 Hardware

4.2.1.1 Processor

A powerful processor is required to handle the computations involved in training and running the model. A multi-core processor can help speed up the training process.

4.2.1.2 Memory (RAM)

A minimum of 8 GB RAM is required for training the model.

4.2.1.3 Graphics Processing Unit

A GPU is required to significantly speed up the training process.

4.2.1.4 Storage

Significant storage space is required for the dataset and the trained model.

4.2.2 Software

4.2.2.1 Python

Python is a high-level programming language that is widely used in various domains of software development, such as web development, data science, artificial intelligence, and scientific computing. Python provides a rich ecosystem for deep learning, with a wide range of libraries and frameworks that make it easy to build and deploy deep learning models.

4.2.2.2 Tensorflow

A free and open-source software library for artificial intelligence and machine learning is called TensorFlow. Although it can be applied to many different tasks, deep neural network training and inference are given special attention. The three components of the Tensorflow structure are preprocessing the data, creating the model, and then training and estimating the model. TensorFlow enables you to design dataflow graphs and structures to express how data moves through a graph by taking inputs as a multi-dimensional array called Tensor. You can use it to make a flowchart of the possible operations that could be carried out on these inputs that go in one direction and out the other.

4.2.2.3 Matplotlib

Matplotlib is a Python 2D plotting library that is used to plot any type of charts in Python. It can deliver figures of publishing quality in a variety of print formats

and interactive settings on many platforms (IPython shells, Jupyter notebooks, web application servers, etc.).

4.2.2.4 pyTorch

Originally created by Meta AI and now a part of the Linux Foundation, PyTorch is a machine learning framework built on the Torch library and used for applications like computer vision and natural language processing. It is open-source software that is available for free under a modified BSD licence. PyTorch features a C++ interface, even though the Python interface is more refined and the main focus of development.

4.2.2.5 NumPy

NumPy is a popular Python library for numerical computations, specifically for scientific computing and data analysis. It stands for "Numerical Python" and is made to offer quick and effective operations on matrices and multidimensional arrays.

4.2.2.6 Pandas

Pandas is an excellent open-source Python toolkit for handling and analysing data. It is frequently used to manage and import datasets. It includes Python data analysis tools that are high-performing and simple to use.

4.3 EXPERIMENTS CONDUCTED

4.3.1 Classification Model

Training and testing the models: Different configurations of CNN, Tuned CNN and HvCNN models were trained and tested on a dataset of MRI scans of breasts.

Hyperparameter tuning: To optimize the performance of the CNN, hyperparameters such as learning rate, batch size, and number of layers were tuned using the PyTorch Gradient Calculation framework.

Comparison of traditional DL CNN, Tuned CNN, and HvCNN: The performance of the traditional DL CNN, Tuned CNN, and HvCNN models were compared to identify which approach provides better results.

4.3.2 Prediction model

Data collection: The Data of breast cancer patients who have experienced relapse and those who have not relapsed were collected.

Data pre-processing: The collected data has been pre-processed to remove noise, missing values, and irrelevant features.

Training and testing the SVM model: An SVM model was trained and tested on the pre-processed data. Different configurations of the SVM model were tested and compared to identify the best-performing model.

Hyperparameter tuning: Hyperparameters of the SVM model such as kernel type, regularization parameter, and gamma were tuned using GridSearchCV to optimize the performance of the model.

Performance evaluation: The performance of the SVM model was evaluated using metrics such as accuracy and ROC Curve.

CHAPTER 5

PERFORMANCE ANALYSIS

5.1 TRADITIONAL DEEP LEARNING CNN

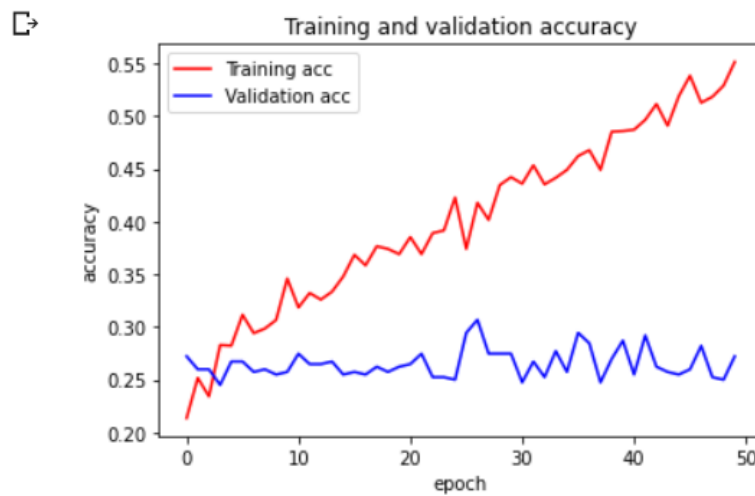


FIGURE 5.1: Graph depicting training and validation accuracy

The training and validation accuracy graph is used for displaying the performance of a machine learning model during training. Two lines are often displayed on the graph: one for the model's accuracy on the training data and the other for its accuracy on a different validation data set. In figure 5.1 we can see that the line for training accuracy increases gradually and the line for validation accuracy increases and decreases erratically.



FIGURE 5.2: Graph depicting training and validation loss

A plot that displays a machine learning model's performance during training is called a training and validation loss graph. It represents a temporal (epoch-based) visualisation of the model's training and validation loss values. The loss value is the difference, for a given input, between the output as predicted by the model and the actual output. The loss value calculated on the training set is known as the training loss, whereas the loss value calculated on the validation set is known as the validation loss. In figure 5.2 we can see that the line for training loss decreases gradually and the line for validation loss increases and decreases erratically.


```
[INFO] accuracy: 27.23%
[INFO] Loss: 1.570113182067871
Time: 0:01:23.710457
```

FIGURE 5.3: Results for the traditional CNN model

MRI images slides at different angles are repetitive and distorted. Accuracy and performance of the model can be considerably increased with improved preprocessing techniques and hyperparameters. Figure 5.3 shows that at present an accuracy of 27.23% is achieved.

5.2 TUNED CNN MODEL

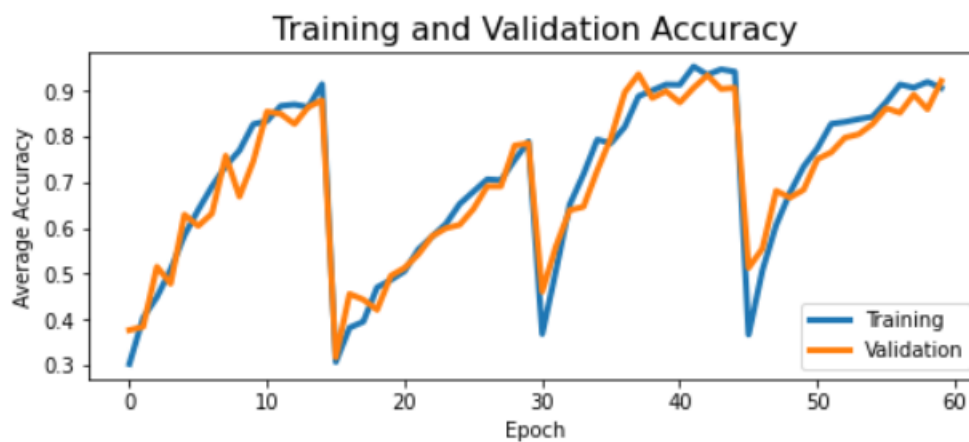


FIGURE 5.4: Graph depicting training and validation accuracy

In figure 5.4 for every 15 epochs the set of hyperparameters change which is why a saw-tooth shape is seen, and we can see that the line for training accuracy and validation accuracy increases gradually for each set.

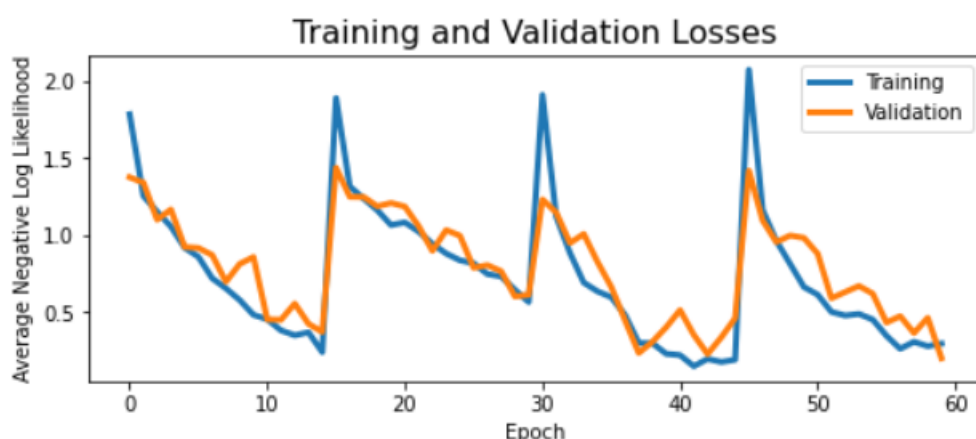


FIGURE 5.5: Graph depicting training and validation loss

In figure 5.5 for every 15 epochs the set of hyperparameters change which is why a saw-tooth shape is seen, and we can see that the line for training loss and validation loss decreases gradually for each set.

	precision	recall	f1-score	support
HER2	0.97	0.94	0.95	201
Luminal	0.96	0.98	0.97	201
Triple	0.90	0.85	0.87	201
ER_PR_HER2	0.84	0.91	0.87	201
accuracy			0.92	804
macro avg	0.92	0.92	0.92	804
weighted avg	0.92	0.92	0.92	804
--Evaluation Metrics--				
Test Accuracy: 0.9166666666666666				
F1 Score: 0.9168057689293903				

FIGURE 5.6: Classification report for the tuned CNN model

Tuning of cnn proved to be efficient. Increased number of epochs and different hyperparameter values will possibly increase the accuracy to great extent. Higher computation power is desirable. Figure 5.6 shows that at present an accuracy of

91.6 % is obtained for the best hyperparameter set of dropout rate = 0.4, learning rate = 0.001, batch size = 25 and hidden units = 512.

5.3 HYPERCOMPLEX VALUED CNN

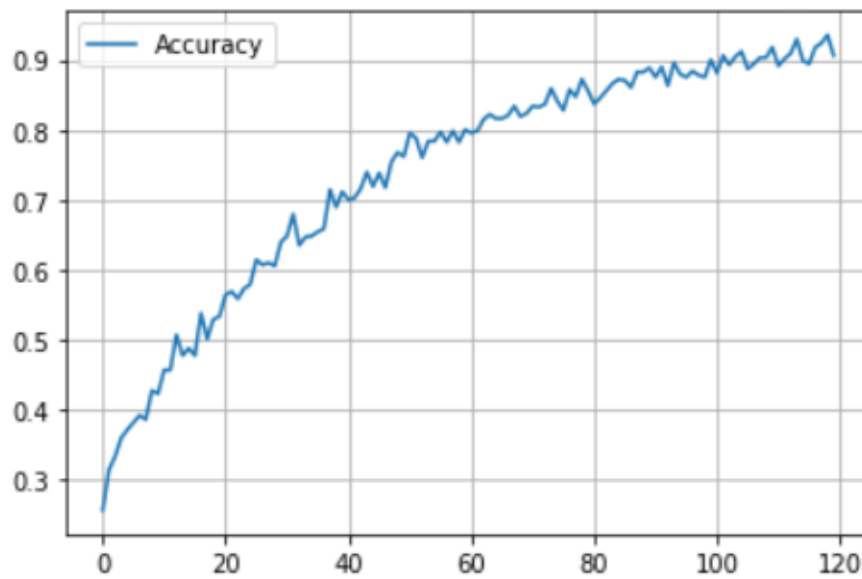


FIGURE 5.7: Graph depicting model accuracy

In figure 5.7 we can see that the line for training accuracy increases gradually.

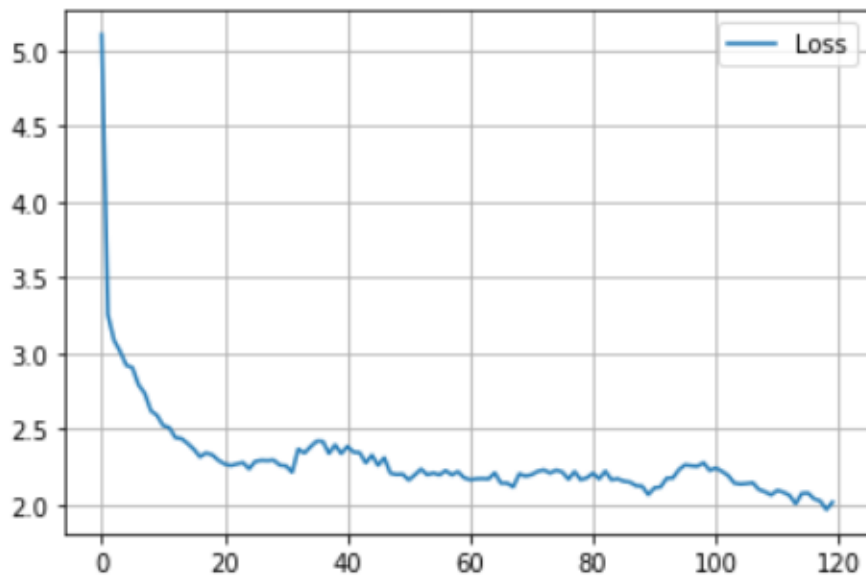


FIGURE 5.8: Graph depicting model loss

In figure 5.8 we can see that the line for training accuracy decreases gradually.

	precision	recall	f1-score	support
Luminal_like	0.92	1.00	0.96	24
HER2	1.00	1.00	1.00	29
ER/PR and HER	1.00	0.97	0.99	35
Triple negative	1.00	0.97	0.98	32
accuracy			0.98	120
macro avg	0.98	0.99	0.98	120
weighted avg	0.98	0.98	0.98	120

FIGURE 5.9: Classification report for the HvCNN model

Figure 5.9 shows that at present an accuracy of 98 % is obtained for HvCNN.

5.3.1 Comparing the performance of Hyperparameter Tuned CNN with HyperComplex-Valued CNN

	Hyperparameter Tuned CNN	Hypercomplex Valued CNN
Accuracy	92%	98%
Precision	92%	98%
Recall	92%	99%
F1-Score	92%	98%

TABLE 5.1: Comparison report

Table 5.1 shows a comparison between HvCNN and Tuned CNN , we see that HvCNN proved to be the better optimization technique providing an accuracy of 98% whereas hyperparamter tuned CNN provided an accuracy of 91.6%.

5.4 RELAPSE PREDICTION MODEL

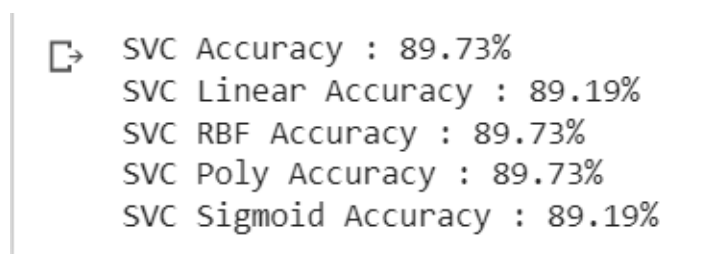


FIGURE 5.10: Performance of the SVM model showing accuracies for different SVMs

The features of the clinical data have been reduced and an SVM model is applied on them to predict relapse. Figure 5.10 shows that it gives an accuracy of 89%

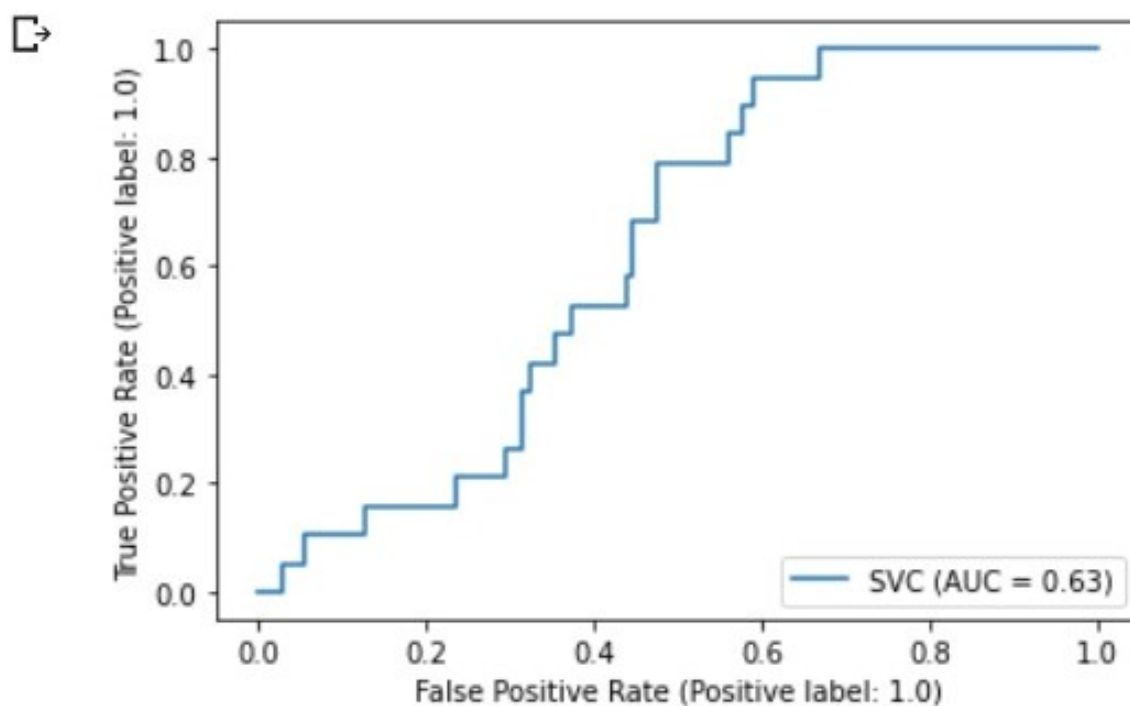


FIGURE 5.11: ROC curve for svm model

Figure 5.11 shows the ROC curve from which we can infer that the area under the curve is 0.63. The classifier can accurately discriminate between all of the Positive and Negative class points when AUC is closer to 1.

	precision	recall	f1-score	support
0.0	1.00	0.98	0.99	166
1.0	0.86	1.00	0.93	19
accuracy			0.98	185
macro avg	0.93	0.99	0.96	185
weighted avg	0.99	0.98	0.98	185

FIGURE 5.12: Classification report for relapse model with GridSearchCV used to optimize hyperparameters for SVM model performance

By optimizing the hyperparameters using GridSearchCV the accuracy has been

considerably increased upto 98% as seen in Figure 5.12.

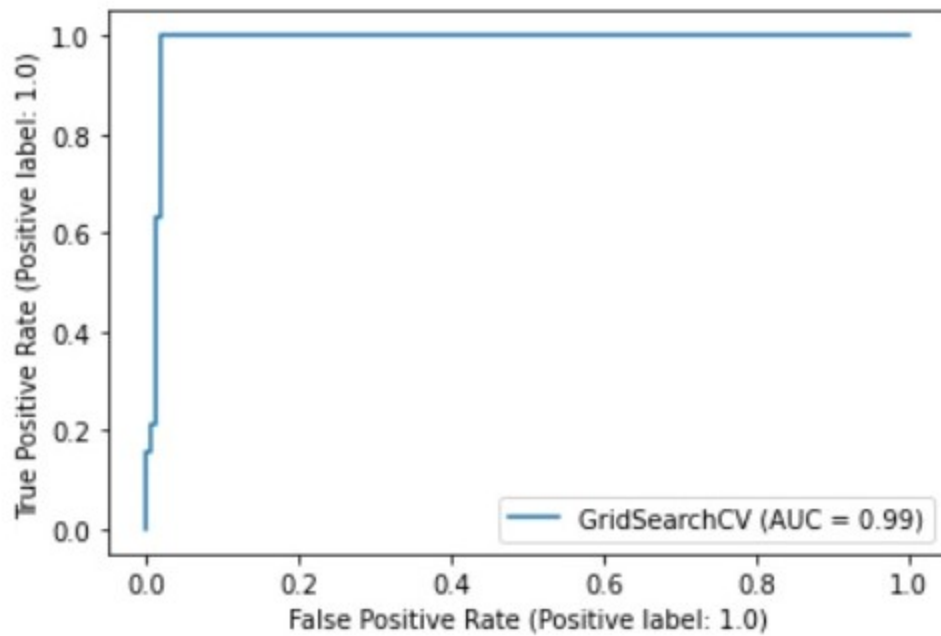


FIGURE 5.13: ROC curve for optimised model using GridSearchCV

Figure 5.13 shows the ROC curve for gridsearch CV from which we can infer that the area under the curve is 0.99 very close to 1.

CHAPTER 6

SOCIAL IMPACT AND SUSTAINABILITY

6.1 APPLICATION IN SOCIETY, HEALTH AND ENVIRONMENTAL ISSUES

Breast cancer imaging plays a major role in reducing the excessive number of deaths due to breast cancer. The system can have a major impact on the society and the health industry as it will speed up the process of detecting breast cancer and give a more accurate prediction thus enabling easier treatment and higher survival rates. The division of breast cancer into molecular subtypes can aid in directing treatment choices and enable the creation of individualised therapy regimens that are catered to the unique features of the tumour. Patients may experience improved outcomes as a result, and reduce unnecessary treatments and their related adverse effects. Breast cancer relapse prediction can offer details about the disease's likely course, which can serve to inform the prognosis and direct patient management. The identification of patients who are more likely to experience a recurrence using this information enables more intensive monitoring and follow-up care. Patients can better understand their risk of recurrence and the factors that contribute to this risk by using a model to predict the recurrence of breast cancer. This may result in better treatment plan adherence and more well-informed decision-making. By lowering the use of chemotherapy and other therapies with adverse environmental effects, the creation of a model to categorise breast cancer into its genetic subtypes may have an effect on the environment. Fewer patients may undergo therapies that are not necessary if personalised treatment plans are available, which would reduce the environmental effect of these treatments.

6.2 SUSTAINABILITY

The research is supported by reliable scientific evidence and concepts. It was created utilising trustworthy datasets that had undergone extensive testing and validation. This guarantees that the model correctly categorises breast cancer into its various molecular subtypes and that clinicians and researchers can use the model. The model is scalable and adaptive by design. The model can be updated and improved as new information becomes available to guarantee that it keeps correctly classifying breast cancer into its molecular subgroups. In developing the model, ethical issues were taken into account. The patient's privacy is respected, and the model is not biased against any certain group. This makes it more likely that patients and medical professionals will trust the model and that it will be long-lasting. Our system's architecture is strong and adaptable, allowing it to take into account changes in the data and categorization standards. The paradigm can be successfully and sustainably incorporated into clinical practise and research.

CHAPTER 7

CONCLUSIONS AND FUTURE WORK

In this work , we have explored various CNN models to classify breast cancer into it's molecular subtypes based on MRI images. The traditional deep learning CNN model achieved an accuracy of 27% , the tuned CNN model achieved an accuracy of 92% and the hypercomplex-valued cnn achieved an accuracy of 98%.We find that the hypercomplex-valued cnn is the ost optimized model to classify breast cancer into it's molecular subtypes.Next, we have explored an SVM model to predict the relapse of breast cancer using clinical data of the patients.The SVM model achieved an accuracy of 89% and on tuning the hyperparameters by using GridSearchCV it achieved and accuracy of 98%.To conclude, we have discussed, in this report, the detailed solution design for classifying breast cancer into their molecular subtypes using state-of-the-art CNN algorithm, the hypercomplex-valued CNN. We also compared the performance of Hyperparameter Tuned CNN with HvCNN. Relapse prediction was performed and accurate results were obtained.

7.1 FUTURE ENHANCEMENTS

The proposed research focuses on using MRI scans for breast cancer diagnosis, but integrating the results with other diagnostic tools such as mammography and biopsy could provide a more comprehensive diagnosis. Furthermore, with the MRI images, the quadrant of the breast in which tumor is located can also be analysed.The work can be extended in the future to perform specific recurrence prediction namely local and distant. With the available clinical data, tumor size, location, staging prediction can also be explored.

REFERENCES

1. Ahmad LG*, Eshlaghy AT, Poorebrahimi A, Ebrahimi M and Razavi AR, Using Three Machine Learning Techniques for Predicting Breast Cancer Recurrence ,J Health Med Inform 2013, DOI: 10.4172/2157-7420.1000124
2. Danish Vasan, Mamoun Alazab, Sobia Wassan, Hamad Naeem, Babak Safaei, Qin Zheng, IMCFN: Image-based malware classification using fine-tuned convolutional neural network architecture, Computer Networks, Volume 171, 2020, 107138, ISSN 1389-1286, <https://doi.org/10.1016/j.comnet.2020.107138>.
3. Eva Tuba, Ivana Strumberger, Ira Tuba, Nebojsa Bacanin, Milan Tuba, Acute Lymphoblastic Leukemia Detection by Tuned Convolutional Neural Network, 32nd International Conference Radioelektronika (RADIOELEKTRONIKA).
doi: 10.1109/RADIOELEKTRONIKA54537.2022.9764909
4. Guilherme Vieira, Marcos Eduardo Valle, Acute Lymphoblastic Leukemia Detection Using Hypercomplex-Valued Convolutional Neural Networks, International Joint Conference on Neural Networks (IJCNN).
doi: 10.1109/IJCNN55064.2022.9892036
5. Jesse Sealand, Joanna Bieniek, Jonathan Tomko , Application of Gradient Boosting Algorithms for Prediction of Relapse in Childhood Acute Lymphoblastic Leukemia , Conference: Pennsylvania Computer and Information Science Educators (PACISE) - Real World Computing
6. J. Margeta, A. Criminisi, R. Cabrera Lozoya, D.C. Lee N. Ayache (2017) Fine-tuned convolutional neural nets for cardiac MRI acquisition

- plane recognition , Computer Methods in Biomechanics and Biomedical Engineering: Imaging Visualization, 5:5, 339-349, DOI: 10.1080/21681163.2015.1061448
7. Jose M. Jerez-Aragones , Jose A. Gomez-Ruiz , Gonzalo Ramos-Jimenez , Jose Muñoz-Perez ,Emilio Alba-Conej A combined neural network and decision trees model for prognosis of breast cancer relapse
 8. Mandeep Rana, Pooja Chandorkar, Alishiba Dsouza, Nikahat Kazi BREAST CANCER DIAGNOSIS AND RECURRENCE PREDICTION USING MACHINE LEARNING TECHNIQUES
 9. Marcos Eduardo Valle, Rodolfo Anibal Lobo , Hypercomplex-Valued Recurrent Correlation Neural Networks December 2020 Neurocomputing 432 DOI:10.1016/j.neucom.2020.12.034
 10. Mustafa Ghaderzadeh, Mehrad Aria, Azamossadat Hosseini, Farkhondeh Asadi, Davood Bashash , Hassan Abolghasemi,A fast and efficient CNN model for B-ALL diagnosis and its subtypes classification using peripheral blood smear images, International Journal of Intelligent Systems · November 2021.
doi: 10.1002/int.22753
 11. Richard Ha, Simukayi Mutasa, Jenika Karcich, Nishant Gupta, Eduardo Pascual Van Sant, John Nemer, Mary Sun, Peter Chang, Michael Z. Liu, and Sachin Jambawalikar Predicting Breast Cancer Molecular Subtype with MRI Dataset Utilizing Convolutional Neural Network Algorithm
 12. Srikanth Tammina , Transfer learning using VGG-16 with Deep Convolutional Neural Network for Classifying Images International Journal of Scientific and Research Publications, Volume 9, Issue 10, October 2019 DOI: 10.29322/IJSRP.9.10.2019.p9420

13. Sungmin Rhee, Seokjun Seo, Sun Kim Hybrid Approach of Relation Network and Localized Graph Convolutional Filtering for Breast Cancer Subtype Classification,IJCAI 2018 <https://doi.org/10.48550/arXiv.1711.05859>
14. Tianwen Xie, Zhe Wang, Qiufeng Zhao, Qianming Bai, Xiaoyan Zhou, Yajia Gu, Weijun Peng and He Wang Machine Learning-Based Analysis of MR Multiparametric Radiomics for the Subtype Classification of Breast Cancer, ORIGINAL RESEARCH article, Front. Oncol., 14 June 2019,Sec. Women's Cancer <https://doi.org/10.3389/fonc.2019.00505>
15. Xiaoli Li, Xuena Li, Yang Xiang, Wenjing Wang, Jun Wang, Jianzhong Wu Breast Cancer Molecular Subtype Classification Using Deep Features
16. Yang Zhang, Jeon-Hor Chen, Yezhi Lin, Siwa Chan, Jiejie Zhou, Daniel Chow,1 Peter Chang, Tiffany Kwong, Dah-Cherng Yeh, Xinxin Wang, Ritesh Parajuli, Rita S. Mehta, Meihao Wang,and Min-Ying Su, Prediction of Breast Cancer Molecular Subtypes on DCE-MRI Using Convolutional Neural Network with Transfer Learning between Two Centers
17. Zhencun Jiang,,Zhengxin Dong,Lingyang Wang,and Wenping Jiang ,Method for Diagnosis of Acute Lymphoblastic Leukemia Based on ViT-CNN Ensemble Model,Volume 2021 — Article ID 7529893 . <https://doi.org/10.1155/2021/7529893>